

This is a self-archived version of an original article. This version may differ from the original in pagination and typographic details.

Author(s): Melander, Marko; Jonsson, Hannes

Title: Effect of H adsorption on the magnetic properties of an Fe island on a W(110) surface

Year: 2019

Version: Published version

Copyright: © 2019 American Physical Society


Rights: In Copyright

Rights url: <http://rightsstatements.org/page/InC/1.0/?language=en>

Please cite the original version:

Melander, M., & Jonsson, H. (2019). Effect of H adsorption on the magnetic properties of an Fe island on a W(110) surface. *Physical Review B*, 100(17), Article 174431.

<https://doi.org/10.1103/PhysRevB.100.174431>

Effect of H adsorption on the magnetic properties of an Fe island on a W(110) surfaceMarko Melander *Department of Chemistry, Nanoscience Center, University of Jyväskylä, FI-40014 Jyväskylä Finland*Hannes Jónsson **Faculty of Physical Sciences, University of Reykjavík, Iceland
and Department of Applied Physics, Aalto University, FI-00076 Aalto, Espoo, Finland* (Received 26 August 2019; revised manuscript received 7 November 2019; published 25 November 2019)

Low-dimensional materials, such as ultrathin films, nanoislands, and wires, are actively being studied due to their interesting magnetic properties and possible technological applications for example in high density data storage. Results of density functional theory calculations within the generalized gradient approximation of an Fe nanoisland on a W(110) surface are presented here with particular focus on the effect of hydrogen adsorption on magnetic properties. The adsorption is found to strongly decrease the magnetic moment of the Fe atoms the H atoms are bound to, down to less than a half in some cases as compared with the clean Fe island. This is an important consideration since hydrogen can relatively easily be introduced and removed from the system, thus providing a way of tuning magnetic properties, and it can also be unintentionally present even under ultrahigh vacuum conditions, especially at low temperature.

DOI: [10.1103/PhysRevB.100.174431](https://doi.org/10.1103/PhysRevB.100.174431)**I. INTRODUCTION**

Low-dimensional structures continue to attract significant attention, partly due to their unique and tunable magnetic properties [1]. Not only can magnetic moments and anisotropy change with size, but low-dimensional magnets can also exhibit more exotic noncollinear spin structures such as skyrmions and helices [1–3]. As the properties are controlled by the atomic structure, it is of both fundamental and technological interest to understand how symmetry, substrate interactions such as strain and dimensionality, among others, affect the magnetic properties.

Of different low-dimensional magnets, ultrathin films and nanoislands of 3d transition metals on paramagnetic substrates have received a great deal of interest. Especially, pseudomorphic iron layers on a W(110) surface has become a common or even archetypical [4] model system of a two-dimensional (2D) magnet. Both monolayer Fe/W(110), Fe nanoislands and stripes of Fe atoms on W(110), can be considered as ideal 2D ferromagnets with high strain (about 11%), large magnetic anisotropy, and coercivity [5] making these structures interesting models for high-density storage [6].

Experimentally, magnetic properties are often studied using a spin-polarized scanning tunneling microscope (STM) [6–9] under ultrahigh vacuum (UHV) conditions. Computational studies based on density functional theory (DFT) are also usually performed in a way that represents vacuum conditions [10,11]. In real systems, however, the magnetic properties are affected by interactions with the environment such as gas adsorption. Hydrogen has been found

to affect the surface magnetism of cobalt [12] and iron [13] 2D magnets. It has also been demonstrated that hydrogen adsorption can induce skyrmionic structure in iridium supported iron overlayers [2]. Both intentional introduction of hydrogen and natural leakage under UHV conditions have been shown to result in similar changes in the coercivity of low-dimension Fe/Pd W-supported magnets [14]. Also, in the presence of oxygen, both adsorption and oxidation can take place [15].

Even under typical UHV conditions at $\sim 10^{-10}$ mbar for several hours, the exposure to gaseous contaminants is inevitable [14,15]. Indeed, molecular hydrogen, the smallest of gases, can leak unintentionally in a seemingly ideal UHV-STM setup [16]. However, little is known about the effect hydrogen adsorption can have on the properties of 2D magnets. This can cause difficulties when interpreting experimental data and when comparing experiments with computational results. On the other hand, intentional addition of hydrogen can offer interesting possibilities for tuning magnetic properties, as mentioned above.

In this work we have performed a systematic DFT study of the effect of hydrogen adsorption on the magnetism of a Fe island on a W(110) support, a typical model system for a 2D ferromagnet. Hydrogen is found to decrease the magnetic moments of neighboring iron atoms by 0.1–0.2 μ_B /H. The magnetic moments initially decrease rather linearly as a function of H-atom coverage while on the fully covered island magnetic moments can decrease by up to 1.25 μ_B compared to the pristine Fe island where the magnetic moment is $\sim 2.7 \mu_B$. The results show and demonstrate that the presence of hydrogen, even under UHV conditions, can significantly change the magnetic properties of 2D magnets.

*hj@hi.is

TABLE I. Surface relaxation and magnetic moments for iron monolayer on a W(110) surface as a function of the number of tungsten layers. Atomic magnetic moments have been computed within the PAW augmentation spheres and are given for the iron monolayer and the first tungsten layer. The total magnetic moment is the amount of spin polarization in the whole system. The unit is Bohr magneton μ_B .

W layers	Relaxation (%)										Magn. Mom. (μ_B)		
	Fe-W	W-W	W-W	W-W	W-W	W-W	W-W	W-W	W-W	W-W	Fe	W	Total
3	-12.9	1.6	0								2.59	-0.14	2.49
4	-12.7	1.2	1.2	0							2.54	-0.15	2.39
5	-12.7	1.8	1.0	1.6	0						2.52	-0.15	2.37
6	-12.6	1.4	1.1	0.9	1.5	0					2.53	-0.15	2.38
7	-12.8	1.3	0.7	0.9	0.9	1.2	0				2.51	-0.15	2.34
8	-13.1	1.5	0.8	0.8	1.2	0.9	1.2	0			2.49	-0.16	2.31
9	-12.9	1.4	1.0	1.0	1.0	1.2	0.9	1.2	0		2.51	-0.15	2.37
10	-13.3	1.2	0.5	0.8	0.9	0.7	1.0	0.6	0.9	0	2.50	-0.16	2.37

II. METHODS

The DFT calculations were carried out using the GPAW [17,18] software within the PAW [19] formalism. Unconstrained KS equations were solved on a real-space grid using 0.2 Å spacing. The spin was relaxed in all calculations. The PBE functional approximation [20] was used. SCF convergence criteria were 10^{-4} eV/electron, 10^{-6} eV, and 10^{-3} electrons for eigenstates, total energy, and electron density, respectively. Convergence criterion for geometry optimization was 0.05 eV/Å.

Calculations of tungsten crystal were first carried out using periodic boundary conditions with $16 \times 16 \times 16$ k -point sampling. The optimized lattice constant is 3.18 Å in good agreement with the experimentally obtained value of 3.16 Å [21]. The epitaxial Fe monolayer on bcc(110) of tungsten was simulated using periodic boundary conditions in xy directions and $16 \times 16 \times 1$ k -point sampling. 10 Å of vacuum was added on both sides of the slab. Convergence of surface relaxation and magnetic moments as a function of tungsten layers was performed and is presented in Table I.

The system was modeled as a three-layer W(110) slab with 10 rows of W atoms in $[\bar{1}10]$ direction and 16 rows in $[001]$ directions as shown in Fig. 1. The slab was periodic in the x - y plane and $2 \times 2 \times 1$ k -point sampling was applied. In total 240 tungsten atoms are included. Two bottom layers were held fixed at the lattice constant 3.18 Å of bulk tungsten, while

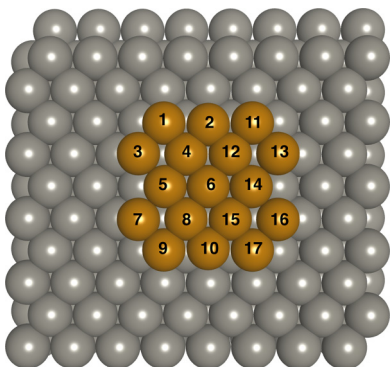


FIG. 1. Epitaxial 7×5 Fe island on bcc(110) surface of tungsten. Iron in orange and tungsten in gray.

the upmost layer was allowed to relax. An epitaxial 7×5 Fe island of 17 atoms was used for studying the magnetism of an Fe nanostructure on the W(110) surface. On each side of the slab 8 Å vacuum was added. To test the adequacy of using three tungsten layers beneath the iron island, a calculation with five layers was also performed. This five-layer model consists of 400 tungsten atoms and is computationally highly demanding. As can be seen in Table II, the three- and five-layer models give similar results. Thus, we have used the three-layer model to study the effect of hydrogen adsorption on the magnetic properties.

Atomic magnetic moments (m_i) were computed as a difference between the number of α and β electrons (n_i^α and n_i^β) within either the PAW augmentation spheres or the Bader regions (V_i) [22] using spin-polarized all-electron densities (ρ^i). The Bader regions and the corresponding electron number of electrons were computed using a grid-based algorithm [23]:

$$m_i = n_i^\alpha - n_i^\beta, \quad (1a)$$

$$n_i^\alpha = \int_{V \in V_i} dV \rho^\alpha(x, y, z). \quad (1b)$$

Interestingly both methods give similar results for the atomic magnetic moments with less than 0.02 μ_B differences which is within the accuracy that can be expected from a DFT/GGA calculation.

III. MAGNETIZATION AND ATOMIC STRUCTURE

A. Full Fe monolayer

Before studying the iron island on tungsten, the properties of an epitaxial iron layer on the W(110) substrate were calculated. Since the surface properties are sensitive to the number of layers used in the slab model, the convergence of relaxation and magnetic moments as a function of the number of tungsten layers was studied. The results are shown in Table I.

The iron layer exhibits a large expansion due to the lattice constant mismatch between iron (2.85 Å) and tungsten (3.18 Å). Introduction of the iron island slightly increased the distances between tungsten layers. From Table I it can be seen that already three tungsten layers capture the relaxation between the iron monolayer and the first tungsten layer. The computed surface relaxations compare well with

TABLE II. Magnetic moments μ_B of an Fe island on a W(110) surface, with and without adsorbed H atoms. The binding sites correspond to the different inequivalent Fe atoms in Fig. 2. The clean Fe island and three-layer W slab is the reference to which other magnetic moments are compared. For example, the absolute magnetic moment for site 1 in the Fe@W5 layers is 2.73 and using the reference convention $\Delta m = 2.73 - 2.75 = -0.02$ given in the table.

Site	Fe@ W three layers	Fe@W five layers	CB	LB	SB	CH	RCH	RH	2H	8H	Rim	Facet rim	Full
1	2.75	-0.02	-0.11	0.05	-0.22	0.04	-0.12	0.02	0.04	-0.16	-0.20	-0.36	-0.51
2	2.76	0.02	0.02	0.02	-0.13	0.04	0.03	-0.19	0.05	-0.09	-0.09	-0.42	-0.50
3	2.68	-0.03	-0.14	-0.09	-0.01	0.01	-0.19	0.01	0.03	-0.11	-0.30	-0.45	-0.37
4	2.60	0.02	-0.03	0.01	0.02	-0.13	-0.02	-0.04	-0.13	-0.14	-0.12	-0.20	-0.16
5	2.47	-0.07	0.00	-0.07	0.02	-0.09	0.04	0.02	-0.06	-0.01	0.07	0.01	-1.26
6	2.61	0.00	-0.02	-0.01	-0.03	0.01	-0.01	-0.01	-0.10	-0.13	-0.11	-0.20	-0.11
7	2.68	-0.03	0.00	0.00	-0.02	0.01	-0.01	-0.01	0.02	-0.12	-0.08	-0.21	-0.12
8	2.60	0.02	-0.01	0.00	-0.01	0.03	-0.02	-0.01	0.04	0.04	-0.11	-0.01	-0.12
9	2.75	-0.02	-0.01	0.03	0.00	0.02	-0.01	0.00	0.02	-0.16	-0.20	-0.38	-0.55
10	2.77	0.02	-0.01	0.01	-0.01	0.01	0.00	-0.01	0.05	-0.10	-0.09	-0.42	-0.54
11	2.75	-0.02	-0.02	0.00	0.01	0.01	-0.01	0.02	0.02	-0.14	-0.21	-0.38	-0.52
12	2.61	0.02	-0.03	0.00	-0.02	0.00	-0.02	-0.05	0.02	0.03	-0.12	-0.01	-0.22
13	2.68	-0.03	-0.01	0.00	-0.01	0.01	-0.01	0.00	0.04	-0.11	-0.30	-0.44	-0.35
14	2.47	-0.07	0.00	0.01	-0.01	0.03	-0.01	0.02	-0.07	0.00	0.07	0.01	-1.24
15	2.61	0.02	-0.02	-0.01	-0.03	0.01	-0.01	-0.01	-0.10	-0.13	-0.11	-0.20	-0.11
16	2.68	-0.03	-0.01	0.00	0.00	0.00	0.00	0.02	0.03	-0.12	-0.08	-0.20	-0.12
17	2.75	-0.02	-0.01	0.00	-0.01	0.00	-0.01	-0.01	0.04	-0.16	-0.20	-0.38	-0.55

the experimentally determined relaxation of 13.0% in the first Fe-W layer [24]. Also the magnetic moments are well presented by the three tungsten layers and are practically converged at five layers of tungsten. The computed magnetic moments are close to the experimentally obtained $2.53 \mu_B$ of Fe-monolayer/W(110) [25] and agree well with previous computational results of Ref. [11].

B. Fe island on W(110)

The iron island was modeled as a 7×5 epitaxial patch of Fe atoms on the W(110) slab. This configuration is labeled as Fe@W island. The Fe@W island has several inequivalent iron atoms which are depicted in Fig. 1. The magnetic moments of each iron atom computed using both the three- and five-layer models are given in Table II. From this table it can be seen that the three- and five-layer models give reasonably consistent magnetic moments for the various Fe atoms. Furthermore, it becomes evident that the atomic magnetic moments depend significantly on the environment and that the environmental effect is local; at the center of the island the atomic magnetic moments are 2.60 – $2.62 \mu_B$, close to the values observed for the full monolayer. At the island rim, Fe atomic magnetic moments are between 2.47 – $2.75 \mu_B$. The iron island is relaxed inwards by -10.4% , slightly less than the full monolayer.

C. H adsorption on the Fe island

The effect of hydrogen adsorption on the magnetic properties of the Fe island was studied by adding one and up to 25 H adatoms. The Fe@W system has several inequivalent adsorption sites for a single hydrogen adatom as depicted in Fig. 2. From Table III it can be seen that hydrogen adsorption is favorable in all the considered sites and the strongest binding occurs at hollow sites in the middle of the island. The nearest neighbor H-Fe bond lengths vary between 1.74

and 1.87 \AA depending on the bonding environment as shown in Fig. 2. Addition of more H adatoms at the central binding sites (2H, see Fig. 3), does not affect the hydrogen adsorption energy even when all the facet sites (8H, see Fig. 3) are populated.

Adsorption of H atoms decreases the magnetic moment of neighboring Fe atoms usually by 0.1 – $0.2 \mu_B$ as is seen from Table II and Fig. 3. This effect is highly local and affects only the Fe atoms adjacent to the H adatom. When several H atoms have been adsorbed on the island, the magnetic moment of the central atoms increases by $0.05 \mu_B$ while atoms at the rims exhibit reduced moments. When several H atoms are bound to an Fe atom, changes in the atomic magnetic moment can be as large as $-1.25 \mu_B$. The effect of multiple adsorbed H atoms on the Fe atomic magnetic moments is nearly additive except for the fully H-covered island.

D. Density analysis of hydrogen induced changes in Fe magnetic moments

Changes in the Fe atomic magnetic moments can be elucidated by studying the density of states obtained by projecting

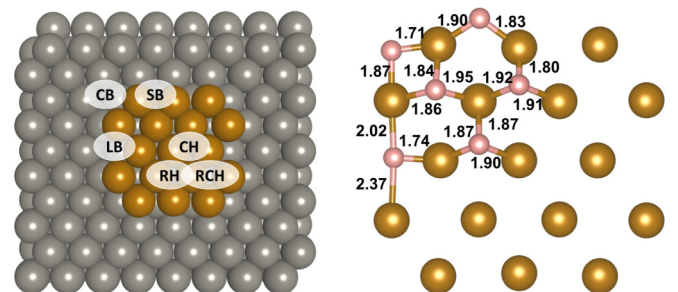


FIG. 2. Left: Hydrogen adsorption sites on the Fe island. Right: Absolute positions of singly adsorbed hydrogen atoms in \AA .

TABLE III. Hydrogen adsorption energy (in eV) for the sites on the Fe island depicted in Fig. 2. The adsorption energy is computed as $E_{\text{ads}} = E_{\text{HFe@W}} - E_{\text{Fe@W}} - 1/2N_{\text{H}}E_{\text{H}_2}$ and in the case of several H adatoms the average adsorption energy $E_{\text{ads}}^{\text{av}} = E_{\text{ads}}/N_{\text{H}}$ is given.

SB	LB	CB	CH	RH	RCH	2H	8H	Rim	8H+rim	Full
-0.51	-0.57	-0.53	-0.72	-0.63	-0.63	-0.71	-0.64	-0.63	-0.58	-0.41

the Kohn-Sham orbitals on atomic orbitals. In Fig. 4 the projected DOS (pDOS) is shown for both the clean and fully H-covered Fe island.

Based on the pDOS analysis it becomes clear that both the up and down states become more populated upon hydrogen adsorption. However, down d states gain more electrons than the up states which explains the observed reduction in atomic magnetic moments. When hydrogen is adsorbed, the d states in general shift to lower energies and the d band becomes wider. While d states are dominating the changes in magnetism, the total change in the atomic magnetic moment is

effectively a sum of changes in d and p states. Both up and down p states gain electrons due to hydrogen adsorption, and the change in magnetic moments caused by the p states varies between -0.05 and $-0.2 \mu_B$. In the total pDOS, the number of states around the Fermi level is reduced as the bands move lower in energy.

IV. DISCUSSION

The data presented above show that the magnetic moments of 2D iron nanomagnets on W(110) are sensitive to the presence of hydrogen. Besides affecting the collinear magnetic structures, as studied here, hydrogen adsorption can also induce noncollinear magnetic states as discussed in the Introduction. While we have not studied noncollinearity in the Fe/W system, earlier theoretical work using a noncollinear extension of the Alexander-Anderson model Hamiltonian (NCAA) concluded that noncollinear states in Fe/W(110) nanomagnets are higher in energy than the collinear states [26,27]. Noncollinear states appeared as unstable transition states between collinear states.

The collinear ground state of the intact Fe/W system does not exclude the possibility of observing noncollinear states in the presence of hydrogen. For instance, the energy from the NCAA Hamiltonian depends on the Coulomb interaction, exchange parameters, and the width of the DOS. These parameters can be extracted by fitting to the atomic magnetic moments, exchange coupling and DOS from DFT calculations [26,27]. In the present work it was shown that hydrogen adsorption leads to significant changes in both magnetic moments and the DOS which in the NCAA would lead to different parameters. It has also been noted that even small changes in NCAA parameters can induce noncollinearity [26]. Hence, it might be possible to infer noncollinearity from a reparametrized NCAA Hamiltonian where hydrogen adsorption is accounted for. The calculations and results presented herein provide a natural starting point for such parametrization of either NCAA or other model Hamiltonians to study noncollinearity that might be induced by hydrogen adsorption.

Beyond model Hamiltonians, it is possible to study noncollinearity using, e.g., noncollinear DFT [28]. Noncollinear DFT captures magnetism from the spin contributions, i.e., the energetics of different relative spin orderings but spin-orbit coupling is needed to capture magnetic anisotropy and the absolute direction of the spin vectors with respect to the underlying atomic lattice. For magnetic 2D nanoislands both the spin and orbital contributions are needed to reliably model noncollinearity in such systems [26]. Accounting for both magnetic contributions in DFT is technically possible (see, e.g., recent work in Ref. [29]) but the achievable system sizes are roughly an order of magnitude smaller than the iron nanoisland considered in the present study.

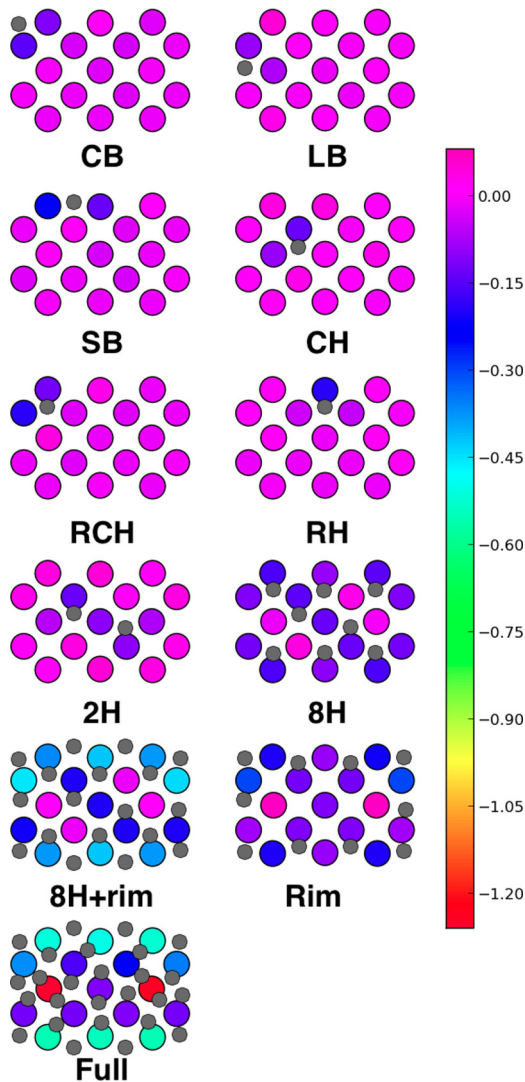


FIG. 3. Changes in the magnetic moments of Fe atoms due to hydrogen adsorption. The gray dots show the position of the hydrogen atoms. The structures are labeled using the same convention as in Tables II and III.

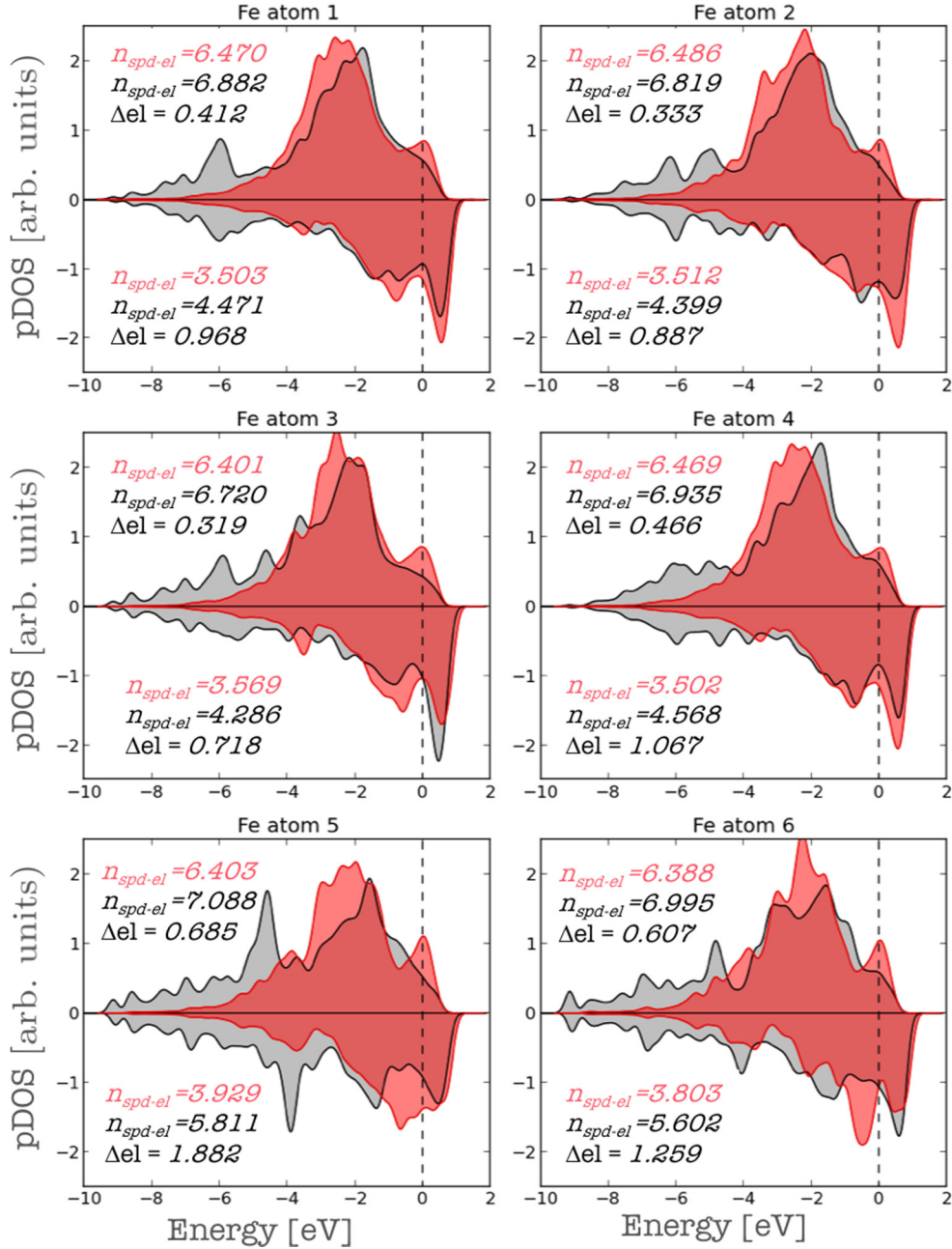


FIG. 4. The projected DOS (pDOS) on the various Fe atoms of Fig. 1 for the clean and fully H-adatom covered Fe island. The red curve and text correspond to the clean island while the black/gray curve and text correspond to the island with H adatoms. n_{spd-el} and Δ_{el} stand for the number and difference in the number of *spd* electrons. The number of electrons is obtained by performing the integral $\int_{-\infty}^{\epsilon_F} d\epsilon \rho(\epsilon)$, where $\rho(\epsilon)$ is the pDOS and $\epsilon_F = 0$ eV is the Fermi level.

Even if hydrogen does not induce noncollinearity, the hydrogen adsorption will dramatically change the magnetic structure of the iron nanoisland. Whether hydrogen adsorption takes place under experimentally relevant conditions can be inferred by studying the surface coverage as a function of hydrogen pressure, temperature, and hydrogen binding energy. For this we use the dissociative Langmuir adsorption isotherm

$$\theta = \frac{\sqrt{KP}}{1 + \sqrt{KP}}, \quad (2)$$

where P is the pressure and K is the equilibrium constant obtained using the adsorption energy with respect to gas phase molecular hydrogen at the relevant temperature and pressure using the ideal gas approximation. In Fig. 5 the surface coverage is reported over a range in temperature and pressure for the weakest (average) hydrogen adsorption energy presented in Table III. This simple analysis shows that an iron nanoisland likely has H adatoms even for the low hydrogen partial pressure and low temperature typically employed in UHV studies of magnetic nanoislands. We emphasize that the

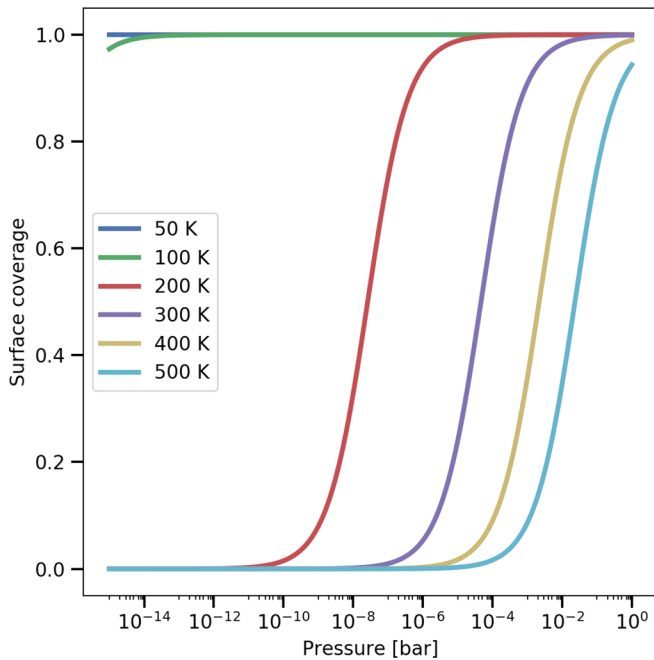


FIG. 5. Hydrogen surface coverage for the “Full” adsorption geometry obtained from the Langmuir adsorption isotherm as a function of the hydrogen pressure and temperature.

presence of hydrogen can also be a way to intentionally tune magnetic properties and is not necessarily a detrimental effect.

V. CONCLUSIONS

The calculations presented here show that hydrogen adsorption can cause a large reduction in the atomic magnetic moment of Fe atoms in nanoislands. Hydrogen atoms bind strongly on both the interior and rim of the Fe island up to high coverage. The magnitude of the change in the magnetic moments depends on the adsorption site. A singly adsorbed hydrogen atom reduces the magnetic moment of the nearest iron atoms by -0.1 to $-0.2 \mu_B$. For a fully H-covered Fe island the magnetic moment is reduced by up to $-1.2 \mu_B$. The effect of hydrogen adsorption on the atomic magnetic moments is highly local affecting only the nearest neighbor Fe atoms. An analysis of the density of states projected on the Fe atoms shows that the changes induced in the magnetic moments are mainly due to filling the minority spin states by hydrogen adsorption. To conclude, the presence of hydrogen can significantly change the electronic structure and magnetic properties of nanoislands and may need to be taken into account when analyzing experimental measurements. It can also be used to intentionally tune magnetic properties of nanoislands.

ACKNOWLEDGMENTS

M.M. acknowledges funding by the Academy of Finland (Project No. 307853). H.J. acknowledges funding from the Icelandic Research Fund. Computational resources were provided by CSC IT CENTER FOR SCIENCE LTD.

There are no conflicts to declare.

- [1] C. A. F. Vaz, J. A. C. Bland, and G. Lauhoff, Magnetism in ultrathin film structures, *Rep. Prog. Phys.* **71**, 056501 (2008).
- [2] K. Nakamura, N. Mizuno, T. Akiyama, T. Ito, and A. J. Freeman, Noncollinear magnetism, magnetocrystalline anisotropy, and spin-spiral structures in Fe/W(110), *J. Appl. Phys.* **101**, 09G521 (2007).
- [3] S. H. Phark, J. A. Fischer, M. Corbetta, D. Sander, K. Nakamura, and J. Kirschner, Reduced-dimensionality-induced helimagnetism in iron nanoislands, *Nat. Commun.* **5**, 5183 (2014).
- [4] M. Ślęzak, T. Ślęzak, K. Freindl, W. Karaś, N. Spiridis, M. Zając, A. I. Chumakov, S. Stankov, R. Ruffer, and J. Korecki, Perpendicular magnetic anisotropy and noncollinear magnetic structure in ultrathin Fe films on W(110), *Phys. Rev. B* **87**, 134411 (2013).
- [5] T. Nakagawa, Y. Takagi, T. Yokoyama, T. Methfessel, S. Diehl, and H.-J. Elmers, Giant magnetic anisotropy energy and coercivity in Fe island and atomic wire on W(110), *Phys. Rev. B* **86**, 144418 (2012).
- [6] D. Coffey, J.-L. Diez-Ferrer, D. Serrate, M. Ciria, C. de la Fuente, and J.-I. Arnaudas, Antiferromagnetic spin coupling between rare earth adatoms and iron islands probed by spin-polarized tunneling, *Sci. Rep.* **5**, 13709 (2015).
- [7] A. Sonntag, J. Hermenau, A. Schlenhoff, J. Friedlein, S. Krause, and R. Wiesendanger, Electric-Field-Induced Magnetic Anisotropy in a Nanomagnet Investigated on the Atomic Scale, *Phys. Rev. Lett.* **112**, 017204 (2014).
- [8] S. Krause, G. Herzog, T. Stapelfeldt, L. Berbil-Bautista, M. Bode, E. Y. Vedmedenko, and R. Wiesendanger, Magnetization Reversal of Nanoscale Islands: How Size and Shape Affect the Arrhenius Prefactor, *Phys. Rev. Lett.* **103**, 127202 (2009).
- [9] E. D. Schaefer, S. V. Chernov, A. A. Sapozhnik, D. M. Kostyuk, A. V. Zaporozhchenko, S. I. Protsenko, M. Bode, S. A. Nepijko, H.-J. Elmers, and G. Schönhense, Morphological and magnetic analysis of Fe nanostructures on W(110) by using scanning tunneling microscopy and Lorentz microscopy, *Jpn. J. Appl. Phys.* **55**, 02BC11 (2016).
- [10] I. Galanakis, M. Alouani, and H. Dreysse, Interface magnetism in ultrathin Fe/W(110) films from first principles, *Phys. Rev. B* **62**, 3923 (2000).
- [11] A. T. Costa, R. B. Muniz, J. X. Cao, R. Q. Wu, and D. L. Mills, Magnetism of an Fe monolayer on W(110), *Phys. Rev. B* **78**, 054439 (2008).
- [12] J. Park, C. Park, M. Yoon, and A.-P. Li, Surface magnetism of cobalt nanoislands controlled by atomic hydrogen, *Nano Lett.* **17**, 292 (2017).
- [13] P. F. Bessarab, V. M. Uzdin, and H. Jónsson, Effect of hydrogen adsorption on the magnetic properties of a surface nanocluster of iron, *Phys. Rev. B* **88**, 214407 (2013).
- [14] C. Chieh-Chen, W.-C. Lin, Y.-C. Yeh, and K.-J. Song, Hydrogen adsorption promoted perpendicular magnetic anisotropy in nano-structured Fe coverage on Pd/W(112) faceting surface, *Appl. Phys. Lett.* **102**, 242403 (2013).

- [15] K. Freindl, E. Partyka-Jankowska, W. Karaś, M. Zając, E. Madej, N. Spiridis, M. Ślęzak, T. Ślęzak, D. Wiśnios, and J. Korecki, Oxygen on an Fe monolayer on W(110): From chemisorption to oxidation, *Surf. Sci.* **617**, 183 (2013).
- [16] F. D. Natterer, F. Patthey, and H. Brune, Quantifying residual hydrogen adsorption in low-temperature STMs, *Surf. Sci.* **615**, 80 (2013).
- [17] J. J. Mortensen, L. B. Hansen, and K. W. Jacobsen, Real-space grid implementation of the projector augmented wave method, *Phys. Rev. B* **71**, 035109 (2005).
- [18] J. Enkovaara, C. Rostgaard, J. J. Mortensen, J. Chen, M. Dułak, L. Ferrighi, J. Gavnholt, C. Glinsvad, V. Haikola, H. A. Hansen, H. H. Kristoffersen, M. Kuisma, A. H. Larsen, L. Lehtovaara, M. Ljungberg, O. Lopez-Acevedo, P. G. Moses, J. Ojanen, T. Olsen, V. Petzold *et al.*, Electronic structure calculations with GPAW: A real-space implementation of the projector augmented-wave method, *J. Phys.: Condens. Matter* **22**, 253202 (2010).
- [19] P. E. Blöchl, Projector augmented-wave method, *Phys. Rev. B* **50**, 17953 (1994).
- [20] J. P. Perdew, K. Burke, and M. Ernzerhof, Generalized Gradient Approximation Made Simple, *Phys. Rev. Lett.* **77**, 3865 (1996).
- [21] M. Fuchs, M. Bockstedte, E. Pehlke, and M. Scheffler, Pseudopotential study of binding properties of solids within generalized gradient approximations: The role of core-valence exchange correlation, *Phys. Rev. B* **57**, 2134 (1998).
- [22] R. Bader, *Atoms in Molecules: A Quantum Theory* (Oxford University Press, Oxford, 1990).
- [23] E. Sanville, S. D. Kenny, R. Smith, and G. Henkelman, Improved grid-based algorithm for Bader charge allocation, *J. Comput. Chem.* **28**, 899 (2007).
- [24] M. Albrecht, U. Gradmann, Th. Reinert, and L. Fritsche, Scattering phases in low energy electron diffraction from spot profile analysis and from multiple scattering theory, *Solid State Commun.* **78**, 671 (1991).
- [25] U. Gradmann, Chapter 1: Magnetism in Ultrathin Transition Metal Films, *Handbook of Magnetic Materials* (Elsevier, Amsterdam, 1993), Vol. 7, pp. 1–96.
- [26] P. F. Bessarab, V. M. Uzdin, and H. Jónsson, Calculations of magnetic states and minimum energy paths of transitions using a noncollinear extension of the Alexander-Anderson model and a magnetic force theorem, *Phys. Rev. B* **89**, 214424 (2014).
- [27] P. F. Bessarab, V. M. Uzdin, and H. Jónsson, Size and Shape Dependence of Thermal Spin Transitions in Nanoislands, *Phys. Rev. Lett.* **110**, 020604 (2013).
- [28] U. von Barth and L. Hedin, A local exchange-correlation potential for the spin polarized case. I, *J. Phys. C: Solid State Phys.* **5**, 1629 (1972).
- [29] S. Haldar, M. Gutzeit, and S. Heinze, Tunneling anisotropic magnetoresistance of Pb and Bi adatoms and dimers on Mn/W(110): A first-principles study, *Phys. Rev. B* **100**, 094412 (2019).